THE ASTROPHYSICAL JOURNAL, 258:683–695, 1982 July 15

THERMONUCLEAR PROCESSES AND ACCRETION ONTO NEUTRON STAR ENVELOPES: X-RAY BURST AND TRANSIENT SOURCES

S. STARRFIELD,[1] S. KENYON,[2] W. M. SPARKS,[3] AND J. W. TRURAN[2]
Received 1981 July 27; accepted 1982 February 1

ABSTRACT

We have used a Lagrangian, fully implicit, one-dimensional, hydrodynamic computer code to investigate the evolution of thermonuclear runaways in the thick, accreted, hydrogen-rich envelopes of 1.0 $M_{\odot}$ neutron stars with radii of 10 km and 20 km. Our simulations produce outbursts which range in time scale from about 2000 seconds to longer than 1 day. Peak effective temperature was 3.3×10^7 K ($kT \sim 2.91$ keV), and peak luminosity was 2×10^5 $L_{\odot}$ for the 10 km study. The 20 km neutron star produced a peak effective temperature and luminosity of 5.3×10^6 K and 5.9×10^2 $L_{\odot}$, respectively. We also investigated the effects of changes in the rates of the ^{14}O(α, p) and ^{15}O(α, γ) reactions on the evolution. Hydrodynamic expansion on the 10 km neutron star produced a precursor lasting about 10^{-6} seconds.

We have also studied the evolution of a gas cloud impacting the surface of a 20 km, 1 $M_{\odot}$ neutron star, in an attempt to simulate the magnetospheric gate model for the X-ray burst sources. This gas is initially at rest with respect to the surface of the neutron star, extends to 185 km above the surface, and is optically thick. The infall resulted in a burst which lasted about 0.1 seconds and reached a peak luminosity and effective temperature of 2.4×10^5 $L_{\odot}$ and 9×10^6 K respectively. The burst was followed by a phase of oscillations with a period of ~ 0.2 seconds.

Subject headings: nuclear reactions — stars: accretion — stars: neutron — X-rays: bursts

I. INTRODUCTION

Significant advances in observational X-ray astronomy have occurred over the past decade. Among the most interesting and exciting new developments have been the discoveries of the X-ray bursters and transient sources. Both of these phenomena involve quiescent X-ray sources which rise abruptly in outburst to a "high" state characterized by a substantially increased X-ray luminosity. The X-ray burst sources typically experience a rapid rise (less than approximately a few seconds) from a "low" state ($\sim 10^{-9}$ ergs cm^{-2} s^{-1}) to a "high" state ($\sim 10^{-7}$–10^{-8} ergs cm^{-2} s^{-1}). This high state generally lasts for 10–20 seconds but may in some instances last for minutes (cf. Grindlay *et al.* 1978; Lewin and Joss 1977; Lewin and Clark 1980). The recurrence time scale for these sources ranges from a few minutes to a few hours, and some objects go through periods of burst activity. The transient X-ray sources have a similar range in observed energy and are characterized by a generally slower rise to a high state which can last from a day to months. For both types of objects, the peak luminosity is assumed to be the Eddington luminosity, $\sim 10^{38}$ ergs s^{-1} for a solar mass object. Excellent reviews of the properties of these objects can be found in Lewin and Joss (1977), Joss (1980), Lamb and Pines (1979), and Lewin and Clark (1980).

The observational evidence suggests that both the X-ray burst and transient sources are associated with some type of instability near the surface of a neutron star (Lewin and Joss 1977; Canizares, McClintock, and Grindlay 1980). This association is supported by a number of theoretical calculations (Hansen and Van Horn 1975; Woosley and Taam 1976; Joss 1977, 1978; Lamb and Lamb 1978; Taam and Picklum 1978, 1979; Taam 1980) which have shown that almost any material except pure hydrogen will burn unstably on a neutron star and produce a thermonuclear runaway.

All of the published studies have described outbursts which resemble the X-ray burst sources rather than the X-ray transient sources. The most recent calculations (Taam 1980) have shown that X-ray bursts can result from accretion of hydrogen-rich material onto a neutron star as well as the helium and carbon used in earlier studies (Joss 1977, 1978; Taam and Picklum 1978). Taam (1980) found short time scale runaways in hydrogen-rich material because the new (larger) rates estimated for the ^{14}O$(\alpha, p)^{17}$F$(p, \gamma)^{18}$Ne and ^{15}O$(\alpha, \gamma)^{19}$Ne reactions (Wallace and Woosley 1981) produced

[1]Department of Physics, Arizona State University; and Theoretical Division, Los Alamos National Laboratory.
[2]Department of Astronomy, University of Illinois.
[3]Laboratory for Astronomy and Solar Physics, NASA Goddard Space Flight Center.

"break-out" from the fast-CN cycle. This resulted in rates of energy generation much larger than could be achieved by the β^+-limited CNO cycle alone (Fowler 1966; Lamb and Lamb 1978).

Given the above results and assuming these two classes of objects are related (Cominsky *et al.* 1978; Lewin and Clark 1980; Fabbiano and Branduardi 1979; Murakami *et al.* 1980; Koyama *et al.* 1981), it is then important to identify those conditions which produce an X-ray transient rather than an X-ray burst. One difficulty in this connection is that the published models of X-ray bursts show that they occur after only $\sim 10^{-12}\ M_\odot$ is accreted. This can produce only $\sim 10^{40}$ ergs from hydrogen burning, and this energy will support the burst luminosities for only 10^2 seconds. One way of prolonging the time scale is to assume very low neutron star luminosities, thus increasing the amount of material that can be accreted. Another possibility is to accrete at such a rate that the hydrogen burns stably and a thick helium shell ignites (Wallace, Woosley, and Weaver 1982). A third possibility, and probably the most important one, is that the kinetic energy of the accreted material is radiated away. For a 10 km neutron star, this energy is $\sim 10^{20}$ ergs g^{-1}. Not only does this amount to 10 times the available nuclear energy, but also the amount of mass that can be involved in the outburst is not limited by the critical mass for a nuclear runaway. Therefore, it is our intent to study a rapid accretion event in this paper in addition to studying thermonuclear runaways in quiescent initial envelopes.

Episodic accretion onto a neutron star was first proposed as a model for the X-ray burst sources by Lamb *et al.* (1977; see also Lamb and Lamb 1978). They predicted that gaseous material would collect at the magnetopause of a neutron star until it cooled sufficiently to break through to the neutron star surface along the field lines. More recent analytic investigations (Baan 1979; Arons and Lea 1980) have studied this instability in some detail and have found that such an event can occur. We will use our Lagrangian, hydrodynamic computer code to study the evolution of this event.

In the following section we discuss our input physics and the various details of our computational techniques. We follow that with a discussion of hydrogen runaways in 10 km and 20 km radius neutron stars (§ III). In the succeeding sections we present the results of our episodic infall simulation (§ IV) and compare our results with observations. We end with a summary and discussion.

II. METHOD OF CALCULATION

In this study we have used a fully implicit, Lagrangian, hydrodynamic computer code (Kutter and Sparks 1972) which incorporates a nuclear reaction network to obtain both the nuclear energy generation and the changes in abundance of the nuclear species (Starrfield *et al.* 1972; Starrfield, Truran, and Sparks 1978; Sparks, Starrfield, and Truran 1978). Since we include only the outermost envelope in the evolutionary studies, we have neglected general relativistic effects. Our equation of state (pressure and energy) and opacity are obtained by interpolation in tabular data kindly provided by Dr. A. N. Cox (Cox and Stewart 1965). For the degenerate regions, we have used the Kippenhahn, Weigert, and Hofmeister (1967) electron-degenerate equation of state to extend the tables. We obtain our degenerate electron conductivities from numerical fits (Sweigert 1973) to the Hubbard and Lampe (1969) tables.

The nuclear reaction rates from the CNO, triple-α, and $^{12}C(\alpha,\gamma)^{16}O$ reactions were taken from Fowler, Caughlan, and Zimmerman (1975), and the rates for the $^{14}O(\alpha,p)^{17}F$ and $^{15}O(\alpha,\gamma)^{19}Ne$ reactions were taken from Woosley (1977, private communication). They are in substantial agreement with those described in Wallace and Woosley (1981). These reactions become important at temperatures greater than 4×10^8 K and allow the conversion of CNO nuclei to higher mass nuclei. However, these rates are rough theoretical estimates and the possibility of future changes should not be ignored (Fowler 1981, private communication). We do not include a full network up to iron because the computer time would be prohibitive. Instead we use the ^{14}O and ^{15}O reactions to provide a measure of the depletion of the CNO nuclei during the evolutionary sequences. We then use this rate of depletion to calculate an energy generation rate by assuming that a few further proton-captures will occur. Our energy generation rates so constructed agree to within a factor of 2 with those determined by Wallace and Woosley (1981) from a more detailed analysis; this discrepancy is of minor consequence when viewed in the light of the order of magnitude uncertainties associated with the ^{14}O-induced and ^{15}O-induced reaction rates themselves.

For the studies to be reported on in § III we began with the hydrogen envelope in place and in thermal and hydrostatic equilibrium. We chose 1.0 $M_\odot$ neutron stars and used radii of 10 km and 20 km to bracket the published work of Joss (1978) and Taam (1980). Although 20 km is somewhat larger than the currently accepted value for the radii of neutron stars (cf. Baym and Pethick 1979; van Paradijs 1979), recent observations of the X-ray burst sources suggest that the radii of the emission regions could be as large as 20 km (Lewin and Clark 1980).

The mass of the hydrogen-rich envelope was increased, in our models, until it reached the critical envelope mass for an outburst. For these models, the temperature structure at any time is determined by the assumed initial luminosity, the time history of the nuclear reactions, and the equations of stellar structure. In the accretion-type studies (cf. Taam 1980), the envelope mass is defined automatically, and its temperature structure at any time is determined by the accretion rate, compressional heating, time history of the nuclear reactions, the equations of stellar structure, and the internal energy that the accreting material has when it is placed on the star. This internal energy is much lower than the kinetic energy of the accreting material (most of which is radiated away), and its value is assumed in the accretion calculations. In both cases, the temperature structure is eventually controlled by the time history of the nuclear reactions, so that the main difference between these procedures is our neglect of compressional heating. The effect of compressional heating decreases as the accretion rate decreases; thus, our models represent a limiting case of accretion-type models for a low accretion rate and low intrinsic neutron star luminosity. The reader should be aware of the fact that both methods must make an assumption concerning the temperature structure at a boundary condition. In our study, it is at the initial time when the internal energy is determined by the assumed initial luminosity of the envelope, and in the accretion-type study it is at the surface interface where the accreted material is given an assumed internal energy. The compatibility of the two procedures is borne out by the fact that our hydrogen-rich envelope mass, $\sim 10^{-11}\ M_\odot$, is only somewhat larger than the value found by Taam (1980). In future studies we will also use the accretion methods and will be able to make a comparison of the two procedures.

In § IV we study an episodic accretion event onto a neutron star. The method that we use has been described by Newman and Cox (1980). In order to simulate the infall, we placed $\sim 10^{-11}\ M_\odot$ of solar composition gas onto the star extending from the surface to a radius of 185 km. The material is initially in thermal equilibrium, optically thick, and at rest with respect to the surface of the star. We initiate the evolution by allowing this gas to begin falling onto the surface.

We include part of the outer edge ($10^{-9} M_\odot$) of the iron core in the computational grid so as to treat correctly the flow of energy into the interior. The remainder of the neutron star is treated as a hard-core inner boundary to the envelope. This allows us to neglect the equation of state of neutron star material (cf. Baym and Pethick 1979). Finally, we assume that all nuclear processing has gone to completion in the interior zones, although neutrino losses are included in these layers; all energy that reaches the innermost zone in our grid is assumed to be radiated by neutrinos.

III. RESULTS OF THE EVOLUTION

In this section we report on the hydrodynamic evolution of thermonuclear runaways in the accreted hydrogen-rich envelopes of neutron stars. We bracket the published studies by choosing radii of 10 km and 20 km. We consider first the case for a 20 km neutron star.

a) *A 20 Kilometer Neutron Star*

The initial conditions for this evolutionary sequence are given in Table 1. For these conditions, virtually the entire accreted envelope has a temperature above 2×10^7 K, and the principal source of energy generation is the CNO reactions. The initial rate of nuclear energy generation is 4×10^{12} ergs g^{-1} s^{-1} at the core-envelope interface (hereafter CEI). The total nuclear energy produced in the envelope exceeds that radiated at the surface by three orders of magnitude, and the temperature begins to increase at a rapid rate. It takes only $\sim 10^3$ seconds for the peak temperature in the envelope to reach 10^8 K; however, this does not occur at the CEI, but rather at a point a few mass shells ($\sim 10^{-12}\ M_\odot$) closer to the surface (Fig. 1). This behavior is caused by the large degenerate electron conductivities in the inner layers, which transport a significant amount of energy into the core at a rapid rate. At about the same time, a

TABLE 1

INITIAL CONDITIONS

Parameter	Sequence 1	Sequence 2	Sequence 3	Sequence 4
Mass ($M_\odot$)	1.0	1.0	1.0	1.0
Radius (km)	20	20	10	185[a]
$M_{\rm ENV}$ ($M_\odot$)[b]	2.0×10^{-11}	2.0×10^{-11}	1.5×10^{-11}	2.0×10^{-11}
$L/L_\odot$	0.1	0.1	0.1	0.1
$\log T_e$	5.8	5.8	5.9	5.3
^{14}O(α, p) and ^{15}O(α, γ) present	yes	no	yes	yes
$T_{\rm CEI}$ (10^7K)	4.1	4.1	4.3	4.5
$\rho_{\rm CEI}$ (g cm^{-3})	4.6×10^5	4.6×10^5	3.1×10^6	2.4×10^2
$\epsilon_{\rm nuc}$ (ergs g^{-1} s^{-1})[c]	4.0×10^{12}	4.0×10^{12}	1.0×10^{14}	1.4×10^9
$\delta R_{\rm H}$ (km)[d]	0.035	0.035	0.022	165.

[a] Initial outer radius of infalling gas. "CEI" stands for core-envelope interface.
[b] Mass of the hydrogen-rich envelope. We assume a solar composition in all models.
[c] Initial rate of energy generation at CEI.
[d] Thickness of envelope.

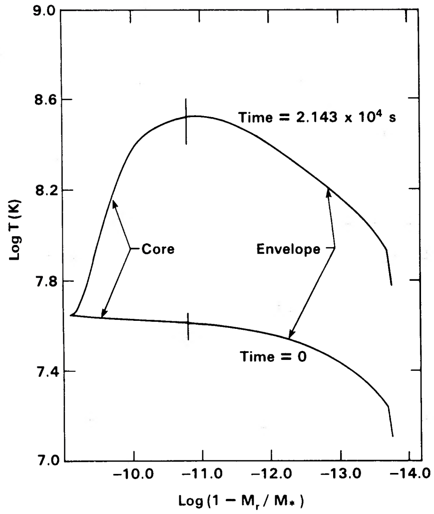

FIG. 1.—This figure shows the temperature structure of the envelope as a function of mass for two times during the evolution of the 20 km neutron star. The vertical bar on each curve marks the core-envelope interface. Time = 0.0 is the initial model; time = 6 hr shows the temperature structure just as the hydrogen abundance is going to zero.

convective region forms above the shell at which peak temperature occurs and slowly grows outward to the surface. The abundances of ^{14}O and ^{15}O have reached 10^{-3} (mass fraction), and both the triple-α reaction and the α-particle reactions on ^{14}O, ^{15}O, and ^{12}C have become important.

The rapid increase in temperature produces an expansion of the envelope, causing it to double in thickness by the time the temperature reaches 3×10^8 K. Although convection retreated as the envelope expanded, it transported enough energy to the surface to raise the luminosity to $10^2\ L_\odot$.

The thermonuclear evolution in the envelope is proceeding as discussed by Taam (1980). The triple-α reaction increases the abundances of the CNO nuclei, which capture protons until they reach ^{14}O and ^{15}O. The α-reactions with ^{14}O and ^{15}O act both to remove CNO nuclei from the CNO reaction sequences and to deplete helium in the region of peak temperature. Because the catalytic nuclei are removed from the CNO reaction sequences, the CNO rates are decreased, and hydrogen remains more abundant than helium. Note that, at these high temperatures ($T > 10^8$), the energy generated by the CNO cycle depends *only* upon the abundance of the CNO catalysts. As a consequence, the CNO reactions are proceeding faster farther out from the CEI, where the temperatures are lower and the ^{14}O and ^{15}O α-reactions are proceeding less rapidly. Therefore, hydrogen is depleted first in a zone about one-third of the way (in mass) to the surface from the CEI (Fig. 2). This occurs about 6 hours after the beginning of the evolution when the luminosity has reached 630 $L_\odot$ and the effective temperature 5.5×10^6 K ($kT \approx 0.5$ keV). Figure 3*a* shows the variation with time of the temperature at the CEI while Figure 3*b* shows the light curve. The rapid initial rise in temperature was caused by the energy production from the ^{14}O(α, p) and ^{15}O(α, γ) reactions. The peak temperature, 4×10^8 K, is not sufficient to drive the CNO nuclei all the way to iron (Audouze, Truran, and Zimmerman 1973; Wallace and Woosley 1981). The energy generation rate peaks at $\sim10^{14}$ ergs g^{-1}s^{-1} and then starts to drop as the helium and CNO nuclei are depleted. The conditions at peak temperature are given in Table 2.

Following hydrogen exhaustion at zone 36, the temperature and luminosity fall precipitously. The entire envelope begins to shrink, causing an increase in density in the interior and accelerating the nuclear reactions. Because of the gradient in the CNO abundances (see above), the hydrogen-burning shell moves inward into the star. As each zone burns out, the temperature and luminosity first fall and then recover, and the shrinkage of the entire envelope keeps the density continuously increasing. A rapid drop and recovery of the effective temperature and surface luminosity occurs as each shell (of gradually increasing mass) is depleted in hydrogen; this is a zoning effect. Because we expect the front to move inward continuously and burn at an average level, we have added a line (see Fig. 3*b*) which we believe traces the result that would have been obtained if the envelope had infinitely fine mass zoning.

The final steep drop in both temperature and luminosity is caused by the burnout of hydrogen at the

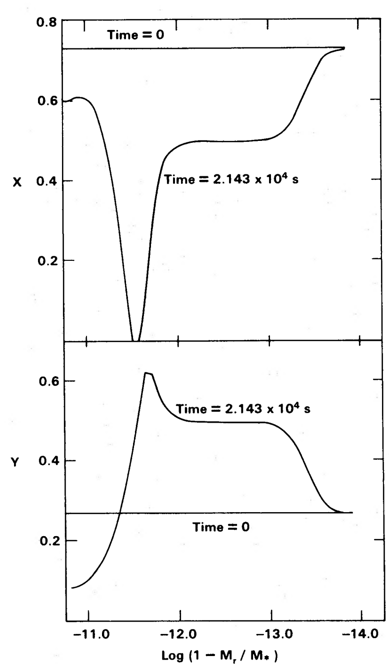

FIG. 2.—The hydrogen (X) and helium (Y) abundances (mass fraction) as a function of mass at two times in the evolution of the 20 km neutron star. The two times are the same as in Fig. 1.

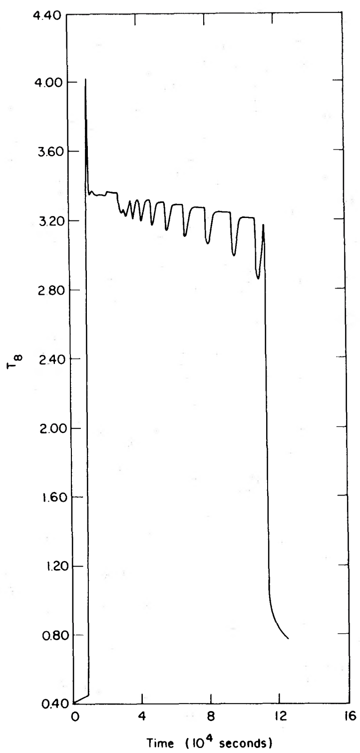

FIG. 3*a*

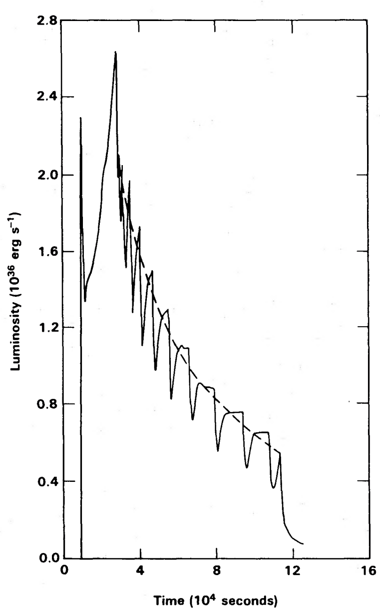

FIG. 3*b*

FIG. 3.—(*a*) The temperature at the zone where peak burning occurs as a function of time for the 20 km neutron star. T_8 is the temperature in units of 10^8 K. The irregularities in this curve are discussed in the text and are caused by coarse zoning. (*b*) The luminosity of the 20 km neutron star as a function of time. The irregularities in the light curve are correlated with those in the temperature plot and are numerical in nature. The dashed line is our expectation of what the actual curve would be if the model had been calculated with finer zoning.

CEI about 1 day after the beginning of the evolution. It will take this sequence some 45 days to return to minimum. Although nuclear burning is still proceeding near the surface, it is insufficient to keep the neutron star hot and luminous. At the end of the evolution, there is approximately 10^{-13} $M_\odot$ of hydrogen on the surface. Below this level, virtually all of the hydrogen and helium have been depleted. One further event occurs because a great deal of energy has been transported into the core. As the outer envelope cools, its luminosity decreases until it reaches about 10^{-2} $L_\odot$. It then begins to rise as the energy in the deeper layers finally reaches the surface. The entire outburst takes about 18 months from the initial state to the final state when the envelope again reaches thermal equilibrium.

b) *Exploring the Influence of the* ^{14}O *and* ^{15}O *Reactions*

The initial conditions for model 2 were identical to those of model 1. However, because of uncertainties in the $^{14}\mathrm{O}(\alpha, p)$ and $^{15}\mathrm{O}(\alpha, \gamma)$ reactions (Wallace and Woosley 1981; Fowler 1981, private communication), we decided to evolve a thermonuclear runaway with these reactions set to zero so that the CNO reactions would be limited by the β^+-decay rates. We found that the character of the outburst was grossly changed by neglecting these rates, suggesting a need for determining the cross sections as accurately as possible.

It takes this sequence about 2000 seconds for the peak temperature in the envelope to exceed 5×10^8 K. The rate of energy generation at this time is $\sim 10^{15}$ ergs g^{-1} s^{-1}. In addition to the CNO reactions, we are getting significant energy generation from the triple-α and $^{12}\mathrm{C}(\alpha, \gamma)^{16}\mathrm{O}$ reactions. In fact, the triple-α reaction is feeding new nuclei into the CNO network, thus enhancing the energy generation. The temperature continues to increase, peaking at a value of $\sim 10^9$ K. At this time the surface luminosity has reached 2.5×10^4 $L_\odot$ and the effective temperature is about 1.3×10^7 K ($kT \approx$ 1.2 keV). The mass fraction of $^{14}\mathrm{O} + {}^{15}\mathrm{O}$ has reached 0.5 and is still climbing as both hydrogen and helium are being depleted at the CEI. The turnover in the temperature is caused by the abundance of hydrogen and helium going to zero at the CEI, and this occurs about 4000 seconds after the beginning of the evolution. Because none of the CNO nuclei are allowed to evolve to higher mass, their abundance reaches $Z_{\mathrm{CNO}} = 0.91$. The thermonuclear runaway now begins its decline, and 2.8 days later the effective temperature has fallen to 10^6 K and the luminosity to 0.7 $L_\odot$. The temperature variation at the CEI with time and the light curve is shown in Figures 4*a* and 4*b*. The small irregularities in the declining portion of each curve are caused by our finite zoning and occur as the hydrogen abundance in each shell vanishes. At the end of the evolution, nuclear burning is still proceeding in the envelope but not at a rate large enough to perturb the flow of energy from the

TABLE 2
PEAK CONDITIONS

Parameter	Sequence 1	Sequence 2	Sequence 3	Sequence 4
T_{CEI} (10^8 K)	4.02	10.0	31.6	14.2
ρ_{CEI} (10^5 g cm^{-3}) ...	2.6	2.4	27.1	2.7×10^{-2}
$L/L_{\odot}$	5.9×10^2	2.5×10^4	8×10^4	2.4×10^5
T_e (K)	5.3×10^6	1.4×10^7	2.6×10^7	8.6×10^6
T_e (keV)	0.46	1.21	2.24	0.74
τ_{rise} (s)[a]	2×10^4	2×10^3	2×10^{-6}	$\sim10^{-4}$
Duration (s)	$\sim1.0\times10^5$	$\sim10^3$	~2000	0.1[b]

[a] Outburst rise time.
[b] Initial peak.

core. The chemical composition of the accreted envelope now consists of ^{13}C, ^{15}N, ^{14}N, ^{17}O, and ^{12}C in the deeper layers, above which lie a thin shell of helium and a tiny surface layer of hydrogen ($\sim10^{-13}$ $M_{\odot}$).

An important result of this evolution is that, contrary to earlier predictions (Lamb and Lamb 1978), hydrogen burning can play a major role in a short time scale runaway even without including the ^{14}O(α, p) and ^{15}O(α, γ) reactions. We find that the triple-α reaction continually feeds new ^{12}C nuclei into the CNO reaction sequence and allows ^{12}C to then capture two protons. Since the β^+-limited CNO cycle has an energy generation rate of

$$\varepsilon_{CNO} = 6\times10^{15} Z_{CNO} \text{ ergs g}^{-1}\text{ s}^{-1}$$

(Fowler 1966), then, as we add CNO nuclei to the reaction sequence, we can raise the rate of energy generation to values exceeding 10^{15} ergs g^{-1} s^{-1}.

c) *A 10 Kilometer Radius Neutron Star*

The initial model had a radius of 9.9 km; the other initial conditions are given in Table 1. The mass of the accreted hydrogen envelope was chosen to be equal to that of the 20 km neutron star in order to determine the effect of the increased gravity on the evolution. It takes this sequence about 130 seconds to evolve to the point where the peak temperature in the shell source reaches 10^8 K. As in the 20 km radius studies, the zone which first flashes to high temperature is not at the CEI but a few zones ($\sim10^{-12}$ $M_{\odot}$) closer to the surface. After 836 seconds of evolution, the temperature in this zone has peaked at 3.3×10^9 K, while the temperature at the CEI has climbed to only 1.95×10^8 K. At the same time, the rate of energy generation exceeds 10^{21} ergs g^{-1} s^{-1}. In contrast to the 20 km evolutionary sequences, the temperature has climbed by nearly 3×10^9 K in 10^{-5} seconds, which causes an overpressure of a few percent in these layers. This produces a shock wave which moves through the envelope and reaches the surface 4×10^{-6} seconds later. As the shock penetrates the surface, the luminosity climbs to 2×10^5 $L_{\odot}$ and the effective temperature reaches 3.3×10^7 K ($kT\approx2.9$ keV). Over the next microsecond the expansion velocities reach 2×10^9 cm s^{-1} but then fall rapidly as the surface expands by less than 1 km in the next 2 microseconds. Figure 5 shows the light curve produced by the shock.

Once the envelope has returned to equilibrium, a nuclear burning front moves both inward and outward from the original shell source. As it passes through each zone, the temperature flashes to values exceeding 10^9 K and the rate of energy generation reaches $\sim10^{22}$ ergs g^{-1} s^{-1}. This intense burst of energy generation comes from the ^{14}O(α, p) and ^{15}O(α, γ) reactions and ends when the ^{14}O and ^{15}O nuclei are depleted in each zone. Unlike the 20 km study, the time scale on which the front moves through the envelope is more rapid than the nuclear burning time scale so that no decrease in luminosity occurs as the energy generation declines in any given zone. The depletion of ^{14}O and ^{15}O effectively shuts off the CNO reactions as an energy source since the abundance of all of the other CNO nuclei have been reduced to values below 10^{-12} (by mass). The only sources of nuclear energy remaining in the envelope are the *p-p* chain and the triple-α reaction.

It takes about 2 seconds for the inward moving burning front to reach the CEI, at which time the temperature in this zone flashes to 3×10^9 K and the rate of energy generation to 10^{22} ergs g^{-1} s^{-1}. Once all of the helium is burned (X is still ~0.4), the rate of energy generation falls rapidly and the internal temperature begins to decline. The evolution of the temperature of the CEI as a function of time is given in Figure 6*a*. The energy from the shell source now penetrates into the outer edge of the core, raising its temperature to values exceeding 10^9 K. If there were any fuel available, possibly from a previous outburst, it would burn on a very short time scale.

As is shown in Figure 5, the light curve drops rapidly after the shock penetrates the surface. The steady burning in the envelope causes a slow but steady return to high luminosities, as is shown in Figure 6*b*. The luminosity reaches 2×10^{38} ergs s^{-1} (which equals L_{Edd}

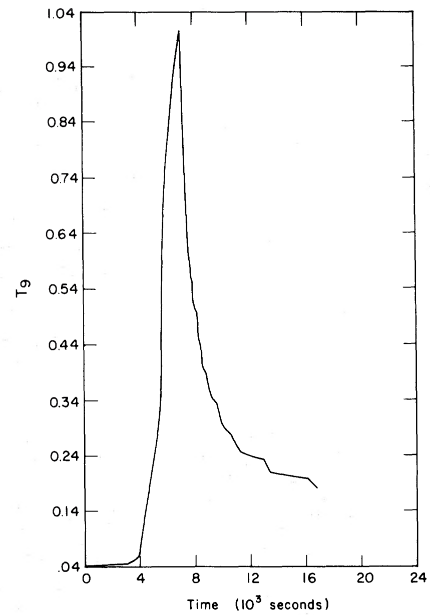

FIG. 4*a*

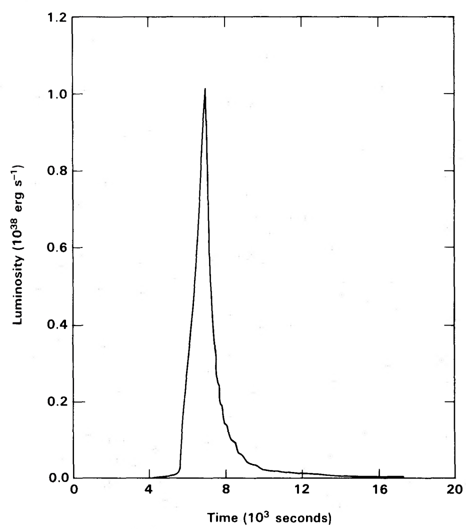

FIG. 4*b*

FIG. 4.—(*a*) The temperature (in units of 10^9 K) as a function of time at the core-envelope interface. This is the 20 km neutron star with the $^{14}O(\alpha, p)$ $^{17}F(p, \gamma)$ ^{18}Ne, and $^{15}O(\alpha, \gamma)$ ^{19}Ne reactions not included. (*b*) The luminosity of the 20 km neutron star without the ^{14}O and ^{15}O α-reactions as a function of time.

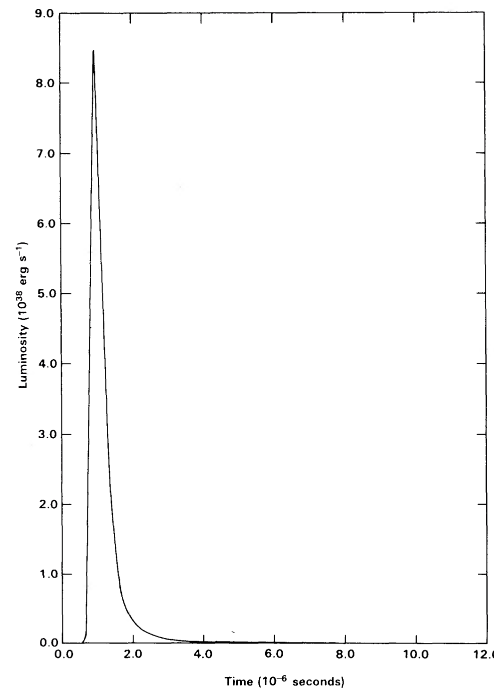

FIG. 5.—The luminosity of the precursor in the 10 km neutron star as a function of time.

for this object), and the surface layers begin to expand at velocities of a few km s^{-1}. Shortly after the envelope reaches a radius of 2×10^8 cm, the envelope becomes pulsationally unstable with excursions in luminosity reaching a factor of 2. Although pulsations originally appeared just after the shock passed through the envelope, they died away as it began expanding to large radii. This new episode of oscillations is extremely interesting in that variations in the luminosity and radius appear correlated with variations in the temperature and, therefore, the rate of energy generation in the shell source. This suggests nuclear energized pulsations. The very irregular appearance of these pulsations in the light curve (*sharp spikes*) shows the results of our attempts to damp them out in order to study the long-term evolution of the thermonuclear runaway. After some 2000 seconds of evolution, the temperature in the shell source has dropped to 1.2×10^9 K and the rate of energy generation to 10^{12} ergs g^{-1} s^{-1}. Inasmuch as most of the energy generation is coming from the *p-p* chain, the nuclear burning time scale has become very long, and it will take many hydrodynamic time steps to complete the evolution.

Therefore, we now begin updating the nuclear abundances and the rate of energy generation after every 10 hydrodynamic time steps. This speeds up the evolution considerably since our computer code spends most of its time inverting the matrix used to solve the nuclear reaction network. Our tests show that the changes in the energy generation do not exceed 1% over 10 hydrodynamic time steps. However, since the rate of energy generation is now constant for a significant number of hydrodynamic time steps, the amplitude of the pulsations drops and the length of the hydrodynamic time steps increases.

During this part of the evolution, the luminosity has oscillated about a value of 5×10^4 $L_\odot$ while the effective

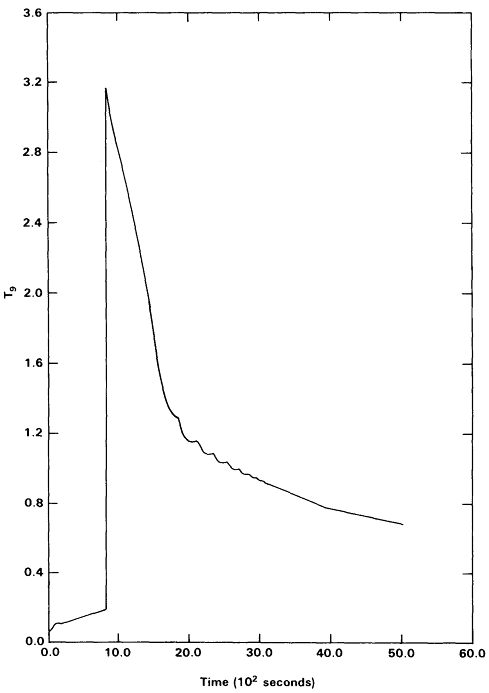

FIG. 6*a*

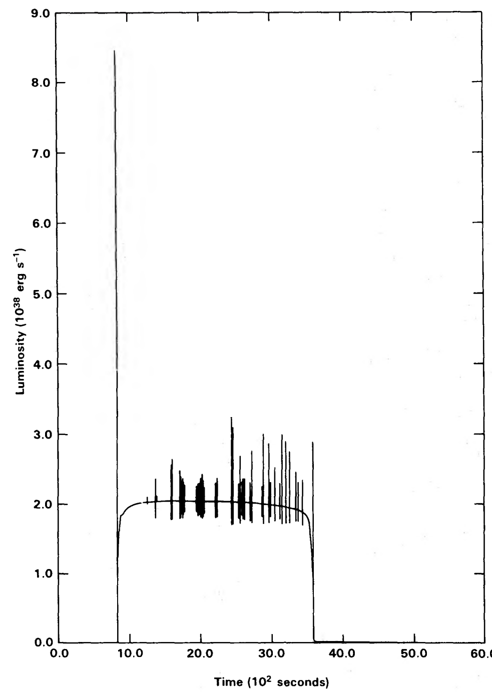

FIG. 6*b*

FIG. 6.—(*a*) The temperature (in units of 10^9 K) at the core-envelope interface as a function of time for the 10 km evolutionary sequence. (b) The luminosity of the 10 km neutron star as a function of time. The initial rise time is on the order of microseconds, and the sharp initial spike is caused by a shock wave penetrating the surface layers. It is shown in detail in Fig. 5. The vertical bars show periods of oscillation of the envelope and these are discussed in the text.

temperature has fallen to $\sim 10^6$ K ($kT \sim 0.1$ keV) as the envelope expanded. This value is much too cool for a normal X-ray burst and the time scale is considerably longer. About 2000 seconds after the initial burst (when the internal temperature has fallen to 8×10^8 K), the envelope starts to shrink and the effective temperature to rise. Because of the release of gravitational energy, the luminosity also rises at this time, reaching a peak value of $\sim 8 \times 10^4\ L_\odot$ before starting its final decline.

The final collapse stage of the evolution takes about 10^2 seconds. As the radius decreases to 5×10^7 cm, the effective temperature climbs to 2.5×10^7 K ($kT \approx 2.2$ keV). The energy emitted in the 2–10 keV range goes through an increase followed by a rapid decrease that would appear as a burst-like behavior in a detector. This behavior is caused both by a change in luminosity and by a shift in the peak of the energy emission. Therefore, for this evolutionary sequence, we would observe two X-ray events separated by a few thousand seconds.

Once the radius has returned to 10 km, the final decline is rapid. It takes the luminosity 10 seconds to fall to $10^3\ L_\odot$ and another 250 seconds to fall to 10^2 $L_\odot$. By this time, the effective temperature has fallen to 5×10^6 K ($kT \sim 0.4$ keV) and the outburst is virtually over. After another 4 hours the luminosity is $\sim L_\odot$. At the end of the evolution, the only nuclear reactions proceeding in the envelope are those converting the remaining hydrogen ($X = 0.3$) to helium on a very long time scale. This result was found also by Taam (1980).

IV. A MODEL WITH ACCRETION

a) *The Burst Phase*

In this calculation, we have used the procedure outlined in § II to simulate an accretion event onto a neutron star. The initial conditions for this sequence can be found in Table 1. The infalling material extended from the surface of the neutron star (20 km) to a radius of 185 km (chosen to keep this gas optically thick). It had an average temperature of $\sim 10^7$ K and a surface luminosity of 0.1 $L_\odot$. As soon as this material begins to fall onto the surface, an accretion shock forms at the boundary. The infall velocities in the envelope reach free fall ($U \sim 2 \times 10^9$ cm s^{-1}) after about 100 μs of evolution when the temperature just behind the shock has climbed to 10^9 K. Over the next few milliseconds, the infalling material passes through the shock, which rapidly moves away from the surface of the neutron star. The outer edge of the gas reaches the accretion shock ~ 3.5 ms after the beginning of the evolution. When the shock finally reaches a radius of 80 km, the entire envelope bounces. The large amount of internal energy produced by the infall is now accelerating the envelope outward which results in the two outermost zones ($M \sim 2\times10^{-14}$ $M_\odot$) achieving escape velocity. The light curve for this part of the evolution is given in Figure 7. A summary of the evolution is given in Table 3. The beginning of the evolution is at the steep rise; the time scale was adjusted to center the burst on the graph. The peak luminosity and effective temperature in the burst reach 2.4×10^5 $L_\odot$ and 9×10^6 K ($kT \sim 0.7$ keV) respectively. While these values are too low for the X-ray burst sources, the surface abundances of the β^+ unstable nuclei exceeded 3×10^{-4} by mass, and the annihilation photons produced during their decay will certainly heat the surface layers (Truran, Starrfield, and Sparks 1978).

The velocities of the surface zones quickly reach 2.8×10^4 km s^{-1}, and both the luminosity and effective temperature fall rapidly as these layers expand. Over the same time period, the envelope has become completely convective and the rate of energy generation at the CEI has reached 10^{18} ergs g^{-1} s^{-1}. It is significantly higher than the equilibrium value of 10^{14} ergs g^{-1} s^{-1} (solar mixture) because convection is carrying fresh CNO nuclei into the burning region and the triple-α process is creating new CNO nuclei. The β^+ unstable nuclei created in the interior are being carried to near the surface where they decay, and this causes the secondary rise in luminosity shown in Figure 6. As the envelope continues to expand, however, the convective zone retreats toward the base of the envelope. Since radiative diffusion cannot efficiently transport energy from the convective region to the surface layers, the surface luminosity continues its rapid decline. The decline in the surface luminosity lasts for another 0.5 seconds until the two escaping zones become optically thin. Once this occurs, radiation from the interior can escape and the luminosity begins to increase. This ends the initial burst of energy.

TABLE 3

EVOLUTION OF THE BURST

Time (ms)	$L/L_\odot$	T_e (K)	Surface Velocity (km s^{-1})
0.0	0.1	2.0×10^5	0.0
1.0	9.6×10^{-2}	2.0×10^5	−3907.0
2.0	8.9×10^{-2}	2.0×10^5	−7965.0
3.0	8.2×10^{-1}	3.6×10^5	−12370.0
4.0	2.5×10^2	1.2×10^6	−17100.0
5.0	2.6×10^3	2.2×10^6	−21170.0
6.0	6.5×10^4	6.8×10^6	+9732.0
7.0	1.7×10^5	8.3×10^6	+21340.0
7.6	2.4×10^5	8.5×10^6	+27660.0
8.0	2.3×10^5	8.1×10^6	+31120.0
9.0	1.4×10^5	6.5×10^6	+36640.0
10.0	9.5×10^4	5.5×10^6	+38180.0
11.0	8.9×10^4	5.0×10^6	+38570.0
12.0	8.9×10^4	4.7×10^6	+38580.0
14.0	9.5×10^4	4.3×10^6	+38270.0
15.6	1.0×10^5	4.0×10^6	+37970.0
20.0	7.2×10^4	3.2×10^6	+37100.0
30.0	4.9×10^4	2.3×10^6	+36110.0
40.0	4.1×10^4	1.9×10^6	+35470.0
50.0	2.8×10^4	1.5×10^6	+35020.0
70.0	1.4×10^4	1.1×10^6	+34460.0
100.0	1.8×10^3	5.4×10^5	+33990.0
130.0	7.0×10^2	3.7×10^5	+33740.0
150.0	3.9×10^2	3.0×10^5	+33620.0
340.0	5.6×10^1	1.2×10^5	+33190.0

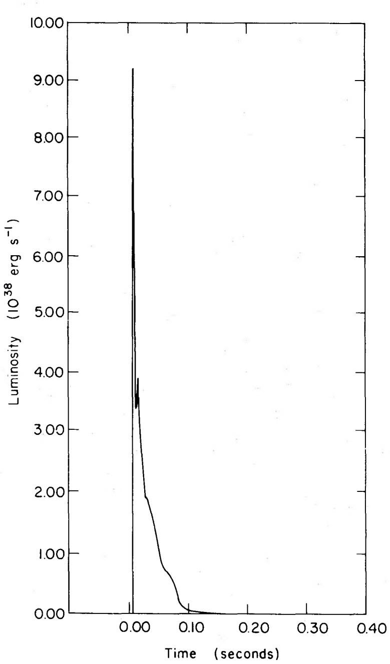

FIG. 7.—The luminosity of the infalling material as a function of time during the initial accretion phase. The beginning of the infall occurs at the beginning of the steep rise; the time scale has been altered to center the burst.

b) The Pulsation Phase

Once the surface layers become optically thin, we find that the entire accreted envelope of the neutron star is pulsating with a period of ~ 0.2 seconds. The light curve for this phase of the evolution is shown in Figure 8. The average luminosity at this time is $\sim 10^4$ $L_\odot$ and the effective temperature is 4×10^6 K ($kT \sim 0.3$ keV). The pulsations are a direct result of the infall (the envelope is ringing) and are not excited by a partial ionization mechanism as in the Cepheid variables. Cox and Hodson (1981, private communication) used the Los Alamos linear nonadiabatic analysis code to test hypothetical neutron star envelopes with boundary conditions taken from our calculations. They found no instability and noted that the pulsations should die out over one to two periods. Since this is certainly not the case, it

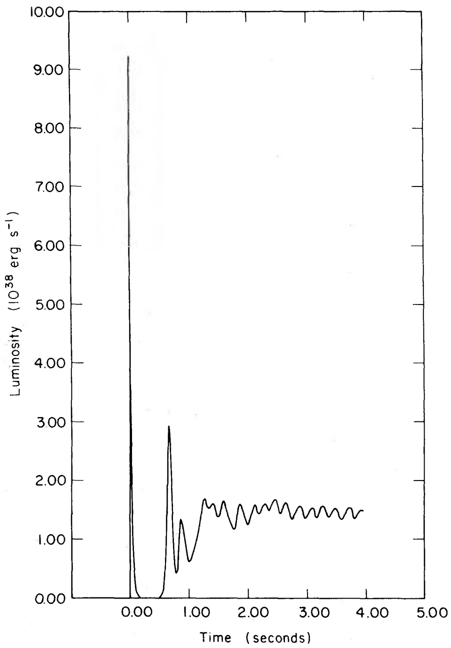

FIG. 8.—The evolution as a function of time of the surface luminosity of the infalling material. An expanded view of the initial spike is given in Fig. 7.

may be that nuclear energy generation is exciting these oscillations. It is also possible that a direct comparison between our calculations and a linear nonadiabatic analysis is not possible because our envelope is far from both hydrostatic and thermal equilibrium. We do not feel that these pulsations are numerical since we took at least 100 time steps per period during this phase of the evolution and because this code has been used previously in a study of Cepheid pulsations (Karp 1975). The peak velocities of these zones are large ($\sim 10^3$ km s^{-1}), and the energy stored in these pulsations is a significant fraction of the energy being radiated by the envelope. We also find that they are occurring in high overtones since the largest velocities occur at the surface and there are a number of nodes present in the interior.

We closely followed these pulsations for ~ 3 seconds. During this interval the temperature and rate of energy generation at the CEI remained unchanged at values of 1.4×10^9 K and 4×10^{18} ergs g^{-1} s^{-1} respectively. We now encountered numerical difficulties because of the large drop in pressure between the two escaping zones (radii $\sim 10^7$ cm) and the interior zones. In order to proceed, we rezoned the envelope by eliminating the escaping, optically thin zones from the computations. This is a standard procedure that has been used previously to study nova remnants (Starrfield, Truran, and Sparks 1978) and has had no effect on the nova evolution when the remaining shells are close to hydrostatic equilibrium. In this case the layers were oscillating, and a short (10 second) transient phase ensued, during which the luminosity of each mass zone decreased and then returned to its pre-rezone value. Nevertheless, the envelope was still pulsating, and we calculated that it would take an additional 10^6 time steps to follow this evolutionary sequence to completion.

c) The Turn-Off Phase

We now evolved three sequences for the purposes of examining the late time evolution. The first included the $^{14}O(\alpha, p)$ and $^{15}O(\alpha, \gamma)$ reactions. The second did not include these reactions, and the third included no nuclear energy generation at all; it was purely a cooling sequence.

In the sequence with the ^{14}O and ^{15}O reactions included, the envelope contracted to a radius of 250 km and then burned quiescently for at least 200 seconds. The luminosity had climbed to 1.7×10^5 $L_\odot$ and the effective temperature reached 1.2×10^7 K ($kT \sim 1.1$ keV). The envelope was completely convective, and the rate of nuclear energy generation ranged from 1.2×10^{18} ergs g^{-1} s^{-1} at the CEI ($T \sim 1.4 \times 10^9$ K) to 10^{11} ergs g^{-1} s^{-1} at the surface. The envelope was shrinking slowly and it would have required a great deal more computer time to follow the resulting evolution, so we ended this calculation. We estimate that it will take ~ 1 day to burn the remaining fuel.

In the sequence with the ^{14}O and ^{15}O reactions absent, the envelope again contracts but then starts to stabilize at ~ 250 km with a luminosity of 1.5×10^5 $L_\odot$ and an effective temperature of 7×10^6 K ($kT \sim 0.6$ keV). We evolved this sequence for about 10^4 seconds, at which point the luminosity was still about 1.5×10^5 $L_\odot$ and the effective temperature was also virtually unchanged. As in the first evolutionary sequence, most of the energy was coming from the triple-α reaction followed by two proton captures. There is enough nuclear fuel for about 1 day of further nuclear energy generation at the current rate of depletion. After that, the luminosity will come solely from contraction and cooling.

The final sequence we evolved was a purely cooling neutron star envelope. We turned off the nuclear reactions but not the neutrino losses. Our initial model was taken at an early stage in the evolution of the previous sequence when its radius was 230 km, its luminosity was 1.4×10^5 $L_\odot$, and its effective temperature was 6×10^6 K. The peak temperature in the envelope had fallen to 9.5×10^8 K. The envelope now begins to contract and, as it contracts, its luminosity and effective temperature increase. After some 200 seconds of cooling, the infall speeds are ~ 0.2 km s^{-1} and the radius is 172 km. It takes 800 seconds for the radius to reach 96 km at which time the luminosity has climbed to 1.6×10^5 $L_\odot$ and the effective temperature is 10^7 K. As the radius continues to decrease, the luminosity and effective temperature slowly increase, as does the time scale for the evolution.

It takes about 40 minutes for the envelope to contract to a radius of 25 km where the luminosity reaches its maximum value of 2×10^5 $L_\odot$. Ninety-three seconds later, the effective temperature reaches its maximum value of 2.17×10^7 K ($kT\sim1.9$ keV). This occurs at a radius of 21.8 km. The luminosity and effective temperature now drop fairly slowly, and it takes about 5–6 days for the neutron star to return to minimum.

V. DISCUSSION

Our calculations of thermonuclear runaways, in combination with the work of Taam (1980; Taam and Picklum 1979), show that it is possible to model the observed behavior of both the X-ray burst and fast transient sources with thermonuclear runaways in the accreted hydrogen-rich envelopes of neutron stars.

a) Nuclear Reactions

An important result of this study is that we were able to obtain outbursts and short time scale phenomena in hydrogen-rich envelopes on neutron stars even in those studies where we did not include the $^{14}O(\alpha, p)$ and $^{15}O(\alpha, \gamma)$ reactions (Audouze, Truran, and Zimmerman 1973; Wallace and Woosley 1981). This is contrary to conclusions drawn by Lamb and Lamb (1978). The reason for this apparent discrepancy is as follows. As noted by these investigators, the maximum rate of energy generation provided by the β^+-limited CNO cycle is $\sim6\times10^{15}$ Z_{CNO} ergs g^{-1} s^{-1} (Fowler 1966). However, we have found in our calculations that, at the temperatures and densities that exist in the envelopes, the triple-α reaction is continuously feeding fresh, unburned nuclei into the CNO reaction sequence. This allows burning rates to exceed 10^{15} ergs g^{-1} s^{-1}. Nevertheless, our runaways are not fast enough to agree with the shortest burst behavior when the $^{14}O(\alpha, p)$ and $^{15}O(\alpha, \gamma)$ reactions are not included in the calculations.

Another interesting result is that the calculation neglecting the ^{14}O and ^{15}O reactions reaches a higher peak temperature and luminosity than the sequence with these reactions present since these reactions rob the CNO network of catalytic nuclei and slow down the rate of nuclear cycling of the CNO reactions. Since our sequence with these reactions present reaches a temperature of only 4×10^8 K, we cannot expect much of the loss in energy to be made up by proton captures on higher mass nuclei (Audouze, Truran, and Zimmerman 1973; Wallace and Woosley 1981). On the other hand, the sequence with the $^{14}O(\alpha, p)$ and $^{15}O(\alpha, \gamma)$ reactions not included reached temperatures of 10^9 K at the CEI. Inasmuch as the cross sections for these rates are somewhat uncertain (Wallace and Woosley; Fowler 1981, private communication), it is important to realize that thermonuclear flashes can be obtained with or without their inclusion. We also found, as did Taam (1980), that most of the hydrogen and all of the helium are consumed during the flash, leaving no residue of fuel for a succeeding flash.

b) The Studies with the Envelope Initially in Equilibrium

Our evolutionary sequences of runaways on 10 km and 20 km radius neutron stars produce theoretical light curves that resemble either the soft X-ray transient sources or the flat-topped X-ray burst sources. They do not, and were not designed to, resemble the short-duration outbursts modeled by Joss (1978) and Taam (1980; see also Taam and Picklum 1979). Our 10 km simulation produced a flat-topped outburst, with a short precursor, that stayed bright for some 2000 seconds. The peak luminosity radiated during the evolution exceeded 2×10^5 $L_\odot$ (8×10^{38} ergs s^{-1}), and its effective temperature exceeded 3×10^7 K ($kT\sim2.8$ keV). The initial flash does not occur at the CEI but at 10^{-12} $M_\odot$ closer to the surface, and then the burning region slowly moves inward. As long as it is moving inward, there is enough energy being produced to keep the star at a constant luminosity. However, once the luminosity reaches the Eddington luminosity, there is a slow expansion of the radius to 2×10^8 cm. The radius remains near this value for nearly the entire duration of the constant luminosity phase before collapsing back down to 10 km at the end of the outburst. While the radius remains at $\sim10^8$ km, the effective temperature decreases below $kT_e\sim0.2$ keV and stays at this value until the radius has returned to 10 km. At this time, the effective temperature then increases back to $kT_e\sim2.2$ keV. Therefore, X-ray observations of this behavior, complicated by shifts in the peak energy of emission, would show two X-ray events separated by about 2000 seconds.

Our 20 km neutron star calculations also showed some interesting behavior. The more luminous object is produced in the calculations carried out without the ^{14}O and ^{15}O reactions present. It is the model where these reactions are included that produced a very irregular light curve which we attribute to finite zoning. The density is low enough that the time scale for the runaway of each interior zone is longer than the cooling time scale of the outer envelope. We expect the burning front to actually move inward smoothly. The evolutionary sequences that we calculated produce outbursts which last from 10^4 seconds (the model with the $^{14}O[\alpha, p]$ and $^{15}O[\alpha, \gamma]$ reactions absent) to 3×10^5 seconds (^{14}O and ^{15}O reactions present). The model with (without) the ^{14}O and ^{15}O reactions reached peak luminosities of 4×10^2 $L_\odot$ (2.4×10^4 $L_\odot$), peak effective temperature of 5×10^6 K (1.4×10^7 K), and peak temperature at the CEI of 4×10^8 K (10^9 K). Our results show that a flat-topped outburst can occur on a neutron star if the outer layers have had enough time to cool from a previous outburst. We can expect these kinds of events to occur and be interspersed between more normal bursts when the mass accretion rate onto the neutron star is reasonably variable. However, our calculations of outbursts on 20 km radii neutron stars produced outbursts which did not become either hot enough or luminous enough to resemble the X-ray burst sources. Nevertheless, their outbursts were not unlike those of the fast, soft, X-ray transient sources recently described by Jensen and Nousek (1980) and Nousek, Cordova, and Garmire (1980). These objects stay bright for about a day and reach peak temperatures of a few million degrees.

c) *Rapid Accretion onto a Neutron Star*

We evolved one sequence where we allowed the material to fall onto the star during the calculations (see also Newman and Cox 1980). We performed this study in an attempt to model the magnetospheric gate hypothesis for the outburst (Lamb *et al.* 1977; Lamb and Lamb 1978).

The burst produced by our sequence was too short ($t \sim 0.1$ s) to agree with the observations of the X-ray burst sources, although it did reach a peak luminosity and effective temperature of 2×10^5 $L_\odot$ and 9×10^6 K respectively. The size of our object, at peak luminosity, is in reasonable agreement with observationally determined radii for some X-ray burst sources (Swank *et al.* 1977; Grindlay *et al.* 1980). Inasmuch as the recent evidence suggests large variations in the intensity and duration of outbursts coming from a single object, and we expect a thermonuclear runaway to produce similar outbursts given *constant* $\dot{M}$, this may be a realistic process for some X-ray burst sources.

The most unusual feature, however, was that the infall set up a "ringing" of the envelope which was still in progress at the end of the computations. Such pulsations have been observed for only one burst (Hayakawa 1981), and our calculations may imply, therefore, that infall is not directly responsible for the outbursts. Analysis of our accreted envelopes with a linear nonadiabatic pulsation code also suggests that no excitation mechanism exists (Cox and Hodson 1981; private communication) and thus the pulsations are a direct result of the accretion event.

Our results in combination with those of other investigators show that the critical envelope mass for a thermonuclear runaway on a neutron star is 10^{-12} $M_\odot$ or smaller. The total energy release possible from this amount of material is $\sim 10^{40}$ ergs and is insufficient to power the outburst of an X-ray transient source. Therefore, we propose that a reasonable model for the X-ray transient outbursts involves an initial outburst of X-rays heating the atmosphere of the secondary and producing a long duration of enhanced mass transfer (Avni, Fabian, and Pringle 1976). The investigations of this phenomenon (Alme and Wilson 1974; see also London, McCray, and Auer 1981) suggest that intense X-ray heating of the secondary will cause mass loss through the inner Lagrangian point. This material will fall into an accretion disk and ultimately onto the surface of the neutron star. One question that must be answered concerns the possibility of observing the energy emitted by accretion between outbursts. If we assume that A0620-00 took ~ 60 years to accrete an envelope with a mass of 10^{-12} $M_\odot$, then the time-averaged mass transfer rate of $\sim 10^{-14}$ $M_\odot$ yr^{-1} implies an X-ray luminosity of $\sim 10^{32}$ ergs s^{-1}. If this object is at a distance of 1 kpc, we would expect a luminosity of $\sim 5 \times 10^{-13}$ ergs cm^{-2} s^{-1}, at the limit of detection of *Einstein Observatory*. Note also that the assumed rate of mass transfer is roughly equivalent to the rate of mass loss by the Sun, so that we do not necessarily have to assume that the secondary of A0620-00 fills its Roche lobe.

The rapid final decline of the light curve of a transient is presumably caused by the termination of mass transfer from the secondary and the emptying out of the accretion disk onto the neutron star. Our calculations of the cooling time scales of hot neutron star envelopes imply that, once burning is ended, the hot envelope cools on time scales of 10^3 seconds or less. This value is in reasonable agreement with the turn-off time scales for the transient and long burst sources. The fact that bursts are not generally associated with the high states of the transients, except for one burst on the decline phase of Cen X-4 (Matsuoka *et al.* 1980) and two bursts in Aql X-1 (Koyama *et al.* 1981), also suggests that the bursts might be a phenomenon associated with low rates of mass transfer onto the neutron star. The similarities between the transient sources at maximum and Sco X-1 suggest that these objects are produced by high rates of mass transfer onto neutron stars.

VI. SUMMARY

The calculations reported on in this paper, in combination with the published studies of Taam (1980) and Taam and Picklum (1979), indicate that the entire range of observed behavior of the X-ray burst and transient sources—time scales and outburst magnitudes—are consistent with thermonuclear runaways in the accreted *hydrogen-rich* envelopes of neutron stars. Our evolutionary study of a runaway on a 10 km neutron star produced an outburst which lasted 2000 seconds and resembled a long-duration burst. It exhibited a precursor, caused by hydrodynamic motions in the envelope, and the hardness of the predicted spectrum varied with time. The outburst on the 20 km radius neutron star lasted about 1 day and may resemble the soft X-ray transient sources.

Energy considerations show that the very longest transient sources (e.g., A0620-00 or Cen X-4) cannot be produced with the amount of material that can be accreted on a neutron star before runaway. We expect that mass transfer must be going on throughout the outburst.

We have also investigated the effects of variations in the (very uncertain) rates of the $^{14}O(\alpha, p)$ and $^{15}O(\alpha, \gamma)$ reactions on the predicted outburst. We found that an outburst can occur, even if the rates of these reactions are significantly lower than estimated. This is due to the fact that convection, acting in combination with the triple-α reaction, serves to keep the CNO reaction sequence far out of equilibrium; these reactions thus produce rates of energy generation far above that predicted for the β^+-limited CNO cycle. All of these models exhausted hydrogen and helium throughout the entire accreted envelope; there was no helium left for further nuclear burning.

We also performed a numerical simulation of the magnetospheric gate theory for the X-ray burst sources (Lamb *et al.* 1977). Rapid mass accretion onto a neutron star produced a burst which lasted ~ 0.1 seconds, but it did not become hot enough to agree with observations of the burst sources. The very rapid burst was followed by a period of oscillations. Nevertheless, our calculations do show that bursts are a possible result of very rapid mass accretion onto a neutron star, and further exploration of this model to produce more realistic bursts is in progress.

We are pleased to acknowledge useful discussions with A. N. Cox, P. Joss, F. Lamb, M. Newman, R. Taam, R. Wallace, S. Woosley, and H. Van Horn. We are also grateful to an anonymous referee whose comments greatly improved the presentation of our results. S. Starrfield thanks George Bell, Stirling Colgate, and Arthur Cox for the hospitality of the Los Alamos National Laboratory and a generous allotment of computer time. G. Atencio did his usual fine job of drawing the figures. This research was partially supported by the National Science Foundation through grants AST 79-21073 to Arizona State University and AST 78-20123 and AST 80-18198 to the University of Illinois.

REFERENCES

Alme, M. L., and Wilson, J. R. 1974, *Ap. J.*, **194**, 147.
Arons, J., and Lea, S. M. 1980, *Ap. J.*, **235**, 1016.
Audouze, J., Truran, J. W., and Zimmerman, B. A. 1973, *Ap. J.*, **184**, 493.
Avni, Y., Fabian, A. C., and Pringle, J. E. 1976, *M.N.R.A.S.*, **175**, 297.
Baan, W. A. 1979, *Ap. J.*, **227**, 987.
Baym, G., and Pethick, C. 1979, *Ann. Rev. Astr. Ap.*, **17**, 415.
Canizares, C. R., McClintock, J. E., and Grindlay, J. E. 1980, *Ap. J. (Letters)*, **236**, L55.
Cominsky, L., Jones, C., Forman, W., and Tananbaum, H. 1978, *Ap. J.*, **224**, 46.
Cox, A. N., and Stewart, J. 1965, *Ap. J. Suppl.*, **11**, 22.
Fabbiano, G., and Branduardi, G. 1979, *Ap. J.*, **227**, 294.
Fowler, W. A. 1966, in *High Energy Astrophysics*, ed. L. Gratton (New York: Academic), p. 328.
Fowler, W. A., Caughlan, G. R., and Zimmerman, B. A. 1975, *Ann. Rev. Astr. Ap.*, **13**, 69.
Grindlay, J. E., *et al.* 1980, *Ap. J. (Letters)*, **240**, L121.
Grindley, J. E., McClintock, J. E., Canizares, C. R., van Paradijs, J., Cominsky, L, Li, F. K., and Lewin, W. H. G. 1978, *Nature*, **274**, 567.
Hansen, C. J., and Van Horn, H. M. 1975, *Ap. J.*, **195**, 735.
Hayakawa, S. 1981, *Space Sci. Rev.*, **29**, 221.
Hubbard, W. B., and Lampe, M. 1969, *Ap. J. Suppl.*, **18**, 297.
Jensen, J., and Nousek, J. 1980, *Bull. AAS*, **12**, 820.
Joss, P. C. 1977, *Nature*, **270**, 310.
———. 1978, *Ap. J. (Letters)*, **225**, L123.
———. 1980, *Ann. N.Y. Acad. Sci.*, **336**, 479.
Karp, A. H. 1975, *Ap. J.*, **199**, 448.
Kippenhahn, R., Weigert, A., and Hofmeister, E. 1967, in *Methods Comput. Phys.*, ed. B. Alder, **7**, 129.
Koyama, K., *et al.* 1981, *Ap. J.*, **247**, L27.
Kutter, G. S., and Sparks, W. M. 1972, *Ap. J.*, **175**, 407.
Lamb, D. Q., and Lamb, F. K. 1978, *Ap. J.*, **220**, 291.
Lamb, F. K., Fabian, A. C., Pringle, J. E., and Lamb, D. Q. 1977, *Ap. J.*, **217**, 197.
Lamb, F. K., and Pines, D. 1979, *Compact Galactic X-Ray Sources* (Urbana-Champaign: University of Illinois Press).
Lewin, W. H. G., and Clark, G. W. 1980, *Ann. N.Y. Acad. Science*, **336**, 451.
Lewin, W. H. G., and Joss, P. C. 1977, *Nature*, **270**, 211.
London, R., McCray, R., and Auer, L. H. 1981, *Ap. J.*, **243**, 970.
Matsuoka, M., *et al.* 1980, *Ap. J. (Letters)*, **240**, L137.
Murakami, T., *et al.* 1980, *Ap. J. (Letters)*, **240**, L143.
Newman, M. J., and Cox, A. N. 1980, *Ap. J.*, **242**, 319.
Nousek, J. A., Cordova, F. A., and Garmire, G. P. 1980, *Ap. J.*, **242**, 1107.
Sparks, W. M., Starrfield, S, and Truran, J. W. 1978, *Ap. J.*, **220**, 1063.
Starrfield, S., Truran, J. W., and Sparks, W. M. 1978, *Ap. J.*, **226**, 186.
Starrfield, S., Truran, J. W., Sparks, W. M., and Kutter, G. S. 1972, *Ap. J.*, **176**, 169.
Swank, J. H., *et al.* 1977, *Ap. J. (Letters)*, **212**, L73.
Sweigert, A. V. 1973, *Astr. Ap.*, **24**, 459.
Taam, R. E. 1980, *Ap. J.*, **241**, 358.
Taam, R. E., and Picklum, R. E. 1978, *Ap. J.*, **224**, 210.
———. 1979, *Ap. J.*, **233**, 327.
Truran, J. S., Starrfield, S., and Sparks, W. M. 1978, in *Gamma Ray Spectroscopy in Astronomy.*, ed. T. Cline and R. Ramaty (NASA Technical Memorandum 79619), p. 315.
van Paradijs, J. 1979, *Ap. J.*, **234**, 609.
Wallace, R. K., and Woosley, S. 1981, *Ap. J. Suppl.*, **45**, 389.
Wallace, R. K., Woosley, S., and Weaver, T. A., 1982, **258**, 696.
Woosley, S., and Taam, R. E. 1976, *Nature*, **273**, 101.

S. Kenyon and J. Truran: Department of Astronomy, University of Illinois, Urbana, IL 61801

W. M. Sparks: Laboratory for Astronomy and Solar Physics, Code 681, NASA Goddard Space Flight Center, Greenbelt, MD 20771

S. Starrfield: Department of Physics, Arizona State University, Tempe, AZ 85287